

Ion–Polymer and Ion–Ion Interactions in Linear Poly(ethylenimine) Complexed with LiCF_3SO_3 and LiSbF_6

Shawna S. York,[†] Morgen Buckner,[‡] and Roger Frech^{*,§}

Division of Natural Science and Mathematics, Oklahoma Baptist University, Shawnee, Oklahoma 74804; College of Mathematics and Science, University of Central Oklahoma, Edmond, Oklahoma 73034; and Department of Chemistry and Biochemistry, University of Oklahoma, Norman, Oklahoma 73019

Received September 12, 2003

ABSTRACT: Systems of linear poly(ethylenimine) (LPEI) complexed with lithium triflate (LiTf), lithium hexafluoroantimonate (LiSbF_6), and tetrabutylammonium hexafluoroantimonate (TbaSbF_6) were studied via FT-IR spectroscopy to determine the changes in ion–polymer and ion–ion interactions that the complexes undergo with changes in salt concentration and temperature. General trends toward loss of order in both the $\text{LPEI}:\text{LiTf}$ and $\text{LPEI}:\text{LiSbF}_6$ systems were noted with increasing temperature as well as increasing salt concentration, leading to the conclusion that an interaction between the polymer and the lithium cation drives the disordering of the two systems. Speciation of the triflate anion was found to be dependent on salt concentration but independent of temperature. In the hexafluoroantimonate systems, the spectral shift of the anion is due to interaction with the polymer rather than interaction with the lithium cation.

Introduction

Limitations in available rechargeable battery technology have resulted in major efforts to develop ion-conducting polymers^{1–12} with high ionic conductivities, good mechanical properties, and thermal, chemical, and electrochemical stability as a highly preferable alternative to the liquid organic electrolytes presently in use. Most fundamental studies of polymer electrolytes have focused on poly(ethylene oxide) complexed with a metal salt.^{1,3,13–19} It is useful to complement this body of work by considering a polymer having a backbone structure similar to that of PEO, but with the oxygen heteroatom replaced with another cation-coordinating heteroatom. Therefore, we have begun studying polymer electrolytes based on linear poly(ethylenimine), LPEI. Structurally this polymer is analogous to PEO in that the oxygen atom of the PEO has been replaced by an NH unit resulting in the monomer repeat unit: $-(\text{CH}_2\text{CH}_2\text{NH})-$. There have been relatively few studies of LPEI–salt complexes. In an earlier paper we used vibrational spectroscopy to study the addition of lithium triflate, LiCF_3SO_3 , and sodium lithium triflate, NaCF_3SO_3 , to LPEI.²⁰ The earliest report of a PEI–polymer electrolyte seems to be a study by Chiang et al. of sodium iodide complexed with PEI.²¹ This was followed by a report from the same authors extending their studies to lithium salts.²² In an early study, Harris et al. described complex formation and ionic conductivity in linear PEI and branched PEI containing NaCF_3SO_3 .^{23,24} Work by Tanaka and co-workers quickly followed.²⁵

It has been recently shown that lithium hexafluoroantimonate, LiSbF_6 , undergoes no cation–anion interactions in PEO systems,²⁶ whereas LiCF_3SO_3 , abbreviated here as LiTf, forms a variety of ionically associated species.^{3,15,27–31} Therefore, it seemed desirable to study

these two limiting cases of ionic association in a novel polymer host, comparing complexes of $\text{LPEI}:\text{LiSbF}_6$ and $\text{LPEI}:\text{LiTf}$. Because cation–anion interactions and cation–polymer interactions are highly dependent on temperature in PEO systems and such interactions are assumed to play an important role in the mechanism of ionic transport, a simultaneous spectroscopic study of these interactions in the LPEI complexes was performed. The results of those investigations are the subject of this paper.

Experimental Section

n-Tetrabutylammonium hexafluoroantimonate (TbaSbF_6) was synthesized by neutralization of fluoroantimonic acid hexahydrate ($\text{HSbF}_6 \cdot 6\text{H}_2\text{O}$) (Aldrich) with *n*-tetrabutylammonium hydroxide (TbaOH) (Aldrich, 1.0 M in water). To ensure that no excess TbaOH would be present, the system was titrated to pH 3.7. Upon addition of TbaOH to the fluoroantimonic acid solution, a white precipitate formed. The precipitate was vacuum-filtered, washed with deionized water, and dried in a vacuum oven for 3 days at 90 °C.

To prepare the electrolytes, LPEI (average MW ca. 21 000) was dried under vacuum at ~70 °C for 24 h. Lithium triflate, LiCF_3SO_3 (LiTf), obtained from Aldrich was dried under vacuum at ~120 °C for 24 h. Anhydrous methanol (99.8%; 0.002% water) from Aldrich was redistilled over sodium. All materials were stored in a nitrogen atmosphere glovebox with moisture less than 1 ppm. Desired ratios of LPEI with LiTf, LiSbF_6 , or TbaSbF_6 were dissolved in anhydrous methanol in the glovebox and stirred for 24 h. The composition of an LPEI–lithium salt system is described by the N:Li molar ratio. To obtain thin films of the samples, the polymer solutions were cast onto zinc selenide IR plates or Teflon sheets, and the methanol was allowed to evaporate at room temperature in the glovebox. The resulting $\text{LPEI}:\text{LiTf}$ films were dried under vacuum for 48 h at ~45 °C. The $\text{LPEI}:\text{LiSbF}_6$ films were dried under vacuum for 48 h at room temperature.

Infrared spectra were recorded with a Bruker IFS66V FT-IR spectrometer over a range of 4000–500 cm^{-1} at a resolution of 1 cm^{-1} . IR spectra of the films were measured between ZnSe plates in an evacuated sample chamber with a temperature-controlled cell over a temperature range from room temperature to 80 °C. A curve-fitting analysis of the spectral data was

[†] Oklahoma Baptist University.

[‡] University of Central Oklahoma.

[§] University of Oklahoma.

* To whom correspondence should be addressed: e-mail rfrech@ou.edu.

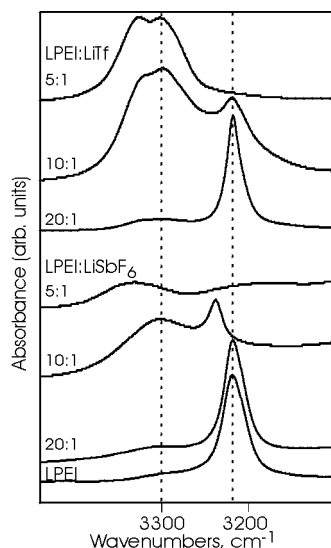


Figure 1. FT-IR spectra of the NH stretching modes of LPEI:LiTf 5:1, 10:1, and 20:1; LPEI:LiSbF₆ 5:1, 10:1, and 20:1; and pure LPEI.

carried out with using a commercial program (Galactic Grams version 5.22). Spectra were curve-fit to a straight baseline and one Gaussian–Lorentzian product function for each band using a nonlinear least-squares method.

Differential scanning calorimetry (DSC) was performed using a Mettler-Toledo DSC820. Thermograms were recorded over a range from -100 to 100 °C at a heating/cooling rate of 5 °C/min.

Results and Discussion

1. NH Stretching Region. Figure 1 shows the composition-dependent IR spectra of the two LPEI–salt systems in the NH stretching region. The NH stretching mode in pure LPEI occurs as a sharp band at 3218 cm^{-1} originating in the crystalline phase of LPEI. This band occurs at a lower frequency than would be expected for a free primary amine due to $\text{N-H}\cdots\text{N}$ hydrogen-bonding interactions. It has been reported by Chatani et al. that the crystal structure of anhydrous LPEI consists of an extensively hydrogen-bonded double helix.³² In the 20:1 LPEI:LiSbF₆ and LPEI:LiTf compositions, there is a weak broad band around 3300 cm^{-1} in addition to the sharp band at 3218 cm^{-1} . In the 10:1 composition in LPEI:LiSbF₆, the broad band at 3300 cm^{-1} becomes more intense, and the sharp band at 3218 cm^{-1} disappears as a sharp band appears at 3238 cm^{-1} . At a 5:1 LPEI:LiSbF₆ composition, the center of the broad, unstructured band has increased to approximately 3375 cm^{-1} , while the sharp band at 3238 cm^{-1} has disappeared. In the 10:1 composition of LPEI:LiTf, the sharp band at 3218 cm^{-1} does not shift but slightly broadens and is lower in intensity, while the broad feature around 3300 cm^{-1} is much more intense. Furthermore, this broad feature is clearly structured, unlike LPEI:LiSbF₆ at this composition, with underlying peaks at 3305 and 3320 cm^{-1} . In the LPEI:LiTf 5:1 spectrum, the sharp peak at 3218 cm^{-1} has disappeared, and the broad peaks have shifted slightly to 3307 and 3325 cm^{-1} . These two bands show that there are at least two spectroscopically distinct hydrogen-bonding environments at high salt concentrations in LPEI:LiTf. The broad bands around 3300 – 3375 cm^{-1} originate in the amorphous phase of the LPEI. The frequency differences between the LPEI:LiTf and LPEI:LiSbF₆ systems indicate a difference not only in the amount but also in the

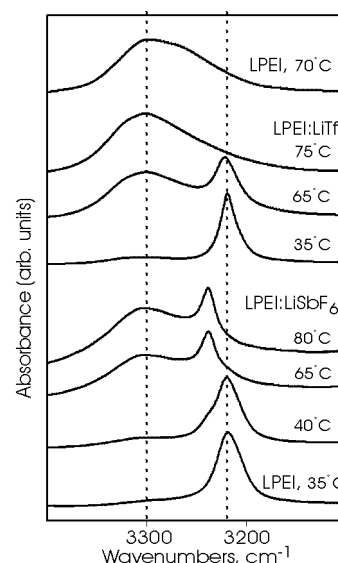


Figure 2. FT-IR spectra of the NH stretching modes of pure LPEI at 70 °C; LPEI:LiTf 20:1 at 75 , 65 , and 35 °C; LPEI:LiSbF₆ 20:1 at 80 , 65 , and 40 °C; and pure LPEI at 35 °C.

nature of the hydrogen-bonding interactions in the two systems.

Temperature-dependent spectra of the NH stretching region for LPEI:LiSbF₆ and LPEI:LiTf, both at a 20:1 composition, are shown in Figure 2. The spectra of LPEI:LiSbF₆ at 40 °C and LPEI:LiTf at 35 °C have a very well-defined, crystalline LPEI band at 3218 cm^{-1} , with both spectra exhibiting a very weak, broad band around 3300 cm^{-1} due to the amorphous phase of the polymer. The LPEI:LiSbF₆ spectrum at 40 °C also has a very weak shoulder at 3238 cm^{-1} . In LPEI:LiSbF₆ at 65 °C the broad structure centered around 3300 cm^{-1} has increased in intensity, the shoulder at 3238 cm^{-1} has become a distinct band of medium intensity, and the peak at 3218 cm^{-1} has disappeared. The LPEI:LiSbF₆ spectrum at 80 °C appears unchanged from 65 °C. In LPEI:LiTf, as the temperature is raised to 65 °C, the broad band at 3300 cm^{-1} increases in intensity as the intensity of the sharp band at 3218 cm^{-1} decreases, until at 75 °C only the broad band around 3300 cm^{-1} remains. The change in band structure with increasing temperature generally resembles the change observed with increasing salt concentration in the LPEI:LiTf system. This behavior is in contrast to the LPEI:LiSbF₆ system, where the sharp band at 3238 cm^{-1} persists above 80 °C and the frequency of the amorphous band is unchanged. For comparison, the spectrum of pure LPEI is shown at room temperature and at 70 °C, which is above the melting temperature of 65 °C. In the 70 °C spectrum, there is a broad band around 3300 cm^{-1} with a lower frequency shoulder. DSC data (not shown) indicate that in both the LPEI:LiTf and LPEI:LiSbF₆ systems the melting peak of crystalline LPEI is much reduced even at a 20:1 salt composition and is completely gone at a 5:1 salt composition. These data taken together with the temperature-dependent IR spectra confirm that the band at 3218 cm^{-1} is due to crystalline LPEI, while the band at 3300 cm^{-1} is due to amorphous LPEI. The shift of the NH stretching band to higher frequencies is expected since crystalline LPEI is extensively hydrogen-bonded. However, the differences in frequencies of the two salt systems at similar compositions and temperatures are noteworthy. The comparison of the concentration-dependent and temperature-de-

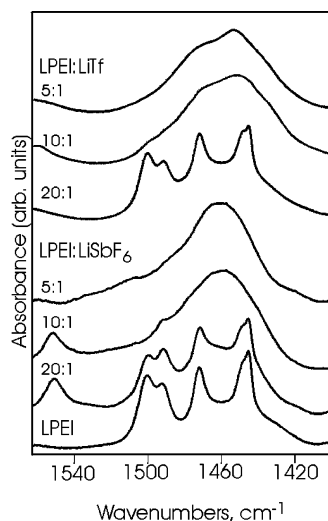


Figure 3. FT-IR spectra of the CH_2 scissoring and NH bending modes of LPEI:LiTf 5:1, 10:1, and 20:1; LPEI:LiSbF₆ 5:1, 10:1, and 20:1; and pure LPEI.

pendent IR data with the DSC data points to the role of the anion, specifically to differences in the interactions of the two anions with the NH group of the polymer. In the LPEI:LiTf system the onset temperature of the melt is unchanged with the addition of salt, whereas in the LPEI:LiSbF₆ system at a 20:1 composition the onset temperature of the melt is reduced by $\sim 15^\circ\text{C}$. In both systems, addition of a sufficient quantity of salt results in the loss of crystallinity; however, in the LiSbF₆ system, there appears to be a competition between $\text{N}-\text{H}\cdots\text{N}$ and $\text{N}-\text{H}\cdots\text{F}$ hydrogen bonds that does not occur in the LiTf system. The disruption of the crystalline structure, either by heating or addition of salt, is accompanied by the breaking of intermolecular $\text{N}-\text{H}\cdots\text{N}$ bonds in both systems, and when sufficient Li^+ is added the system is completely amorphous.

2. CH_2 Scissors and NH || Bending Region and CH_2 Twisting and NH || Bending Region. Modes between 1560 and 1420 cm^{-1} (shown in Figure 3) are comprised of a mixture of CH_2 scissoring and NH bending parallel to the chain axis.³³ In pure LPEI and 20:1 LPEI:LiSbF₆, there are well-defined bands at 1500 , 1491 , 1472 , and 1445 cm^{-1} , with a shoulder at 1448 cm^{-1} . A high degree of disordering in both LPEI:LiSbF₆ and LPEI:LiTf occurs in the composition range between 20:1 and 10:1. In the 10:1 and 5:1 LPEI:LiTf samples there are two broad, overlapping peaks at roughly 1460 and 1480 cm^{-1} that originate from the LPEI peaks at 1445 and 1472 cm^{-1} . In the 10:1 sample of LPEI:LiSbF₆ there is a broad band at 1460 cm^{-1} with a shoulder at 1490 cm^{-1} that is markedly decreased in the 5:1 composition. In the LPEI:LiSbF₆ at the 20:1 and 10:1 compositions, a new band appears at 1550 cm^{-1} which disappears in the 5:1 composition. This band probably arises from an NH bending mode occurring at 1500 cm^{-1} in pure LPEI that is shifted due to a hydrogen-bonding interaction with the SbF_6^- anion.

The temperature-dependent spectra in the same region are shown in Figure 4. The overall temperature-dependent trends observed here in both LPEI:LiSbF₆ and LPEI:LiTf spectra are also seen in the spectral regions from ~ 800 to 1100 cm^{-1} : well-defined bands at lower temperatures followed by extensive disordering of the system between 40 and 65°C . As in the other regions, this behavior bears a remarkable resemblance

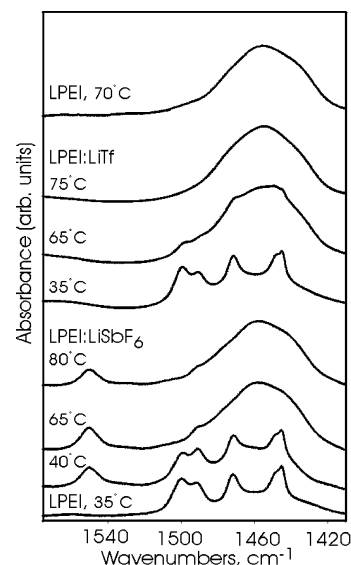


Figure 4. FT-IR spectra of the CH_2 scissoring and NH bending modes of pure LPEI at 70°C ; LPEI:LiTf 20:1 at 75 , 65 , and 35°C ; LPEI:LiSbF₆ 20:1 at 80 , 65 , and 40°C ; and pure LPEI at 35°C .

to the disordering that occurs upon increasing the salt concentration from a composition of 20:1 to 10:1. The increase in intensity of the peak at 1490 cm^{-1} when LiSbF₆ is added to the system was noted in Figure 3. This band persists at 65 and 80°C where the remainder of the band structure is disrupted. Note the peak at 1550 cm^{-1} in the LPEI:LiSbF₆ spectra.

In both the NH stretching region (Figures 1 and 2) and the NH bending region (Figures 3 and 4), bands appear in the 20:1 and 10:1 LPEI:LiSbF₆ composition which persist above the melt for the 20:1 but which do not appear in the 5:1 composition. The appearance of bands of significant intensity in LPEI:LiSbF₆ and the absence of corresponding bands in pure LPEI or LPEI:LiTf suggest a significant interaction between the SbF_6^- anion and the NH group of the host polymer. The disappearance of these bands at a salt concentration of 5:1 suggests a hydrogen-bonding interaction between the fluorine atom of the anion and the NH group of the polymer that is then disrupted by an interaction with the lithium cation.

The spectral region between 1070 and 1010 cm^{-1} contains modes that are a complex mixture of the CH_2 twisting, rocking, and wagging and NH in-plane bending vibrational motions.³³ As in the region from 1560 to 1420 cm^{-1} , there is extensive coupling between the CH_2 and NH bending modes. In pure LPEI at room temperature, there is a well-defined band at 1049 cm^{-1} and a weak, broad band centered at 1023 cm^{-1} . In the LPEI:LiSbF₆ system, as either the salt concentration or the temperature is increased, the band at 1049 cm^{-1} disappears, and the broad weak band shifts to 1037 cm^{-1} (data not shown). In the LPEI:LiTf 20:1 spectrum, the LPEI band at 1049 cm^{-1} disappears above the polymer melting temperature, leaving only the $\nu_s(\text{SO}_3)$ band of the triflate anion. The spectrum of pure LPEI at 70°C shows no band at all in this region.

3. CH_2 Rocking and NH \perp Bending. The concentration-dependent IR spectra of LPEI:LiSbF₆ and LPEI:LiTf from ~ 900 to 750 cm^{-1} are shown in Figure 5. Modes in this region are a mixture of NH out-of-plane bending and CH_2 rocking motions.³³ These modes have been shown to be sensitive to changes in the polymer

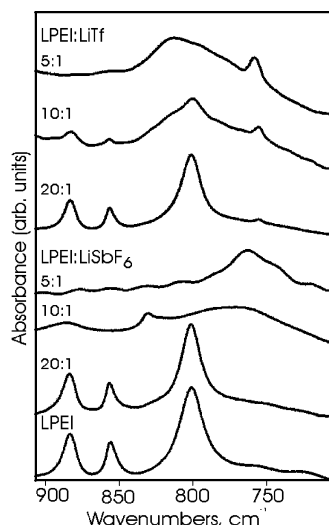


Figure 5. FT-IR spectra of the NH out-of-plane bending and CH_2 rocking modes of LPEI:LiTf 5:1, 10:1, and 20:1; LPEI:LiSbF₆ 5:1, 10:1, and 20:1; and pure LPEI.

conformation.^{33,34} In pure LPEI and 20:1 LPEI:LiSbF₆, there are well-defined bands at 883, 855, and 800 cm^{-1} . As the salt content is increased to a 10:1 composition, the band at 800 cm^{-1} becomes very broad and shifts to 770 cm^{-1} . The band at 883 cm^{-1} also broadens and undergoes a slight shift to 885 cm^{-1} . The new band at 829 cm^{-1} may originate in the medium intensity band at 855 cm^{-1} in the pure LPEI spectrum, but it is noticeably less broadened than the other bands in this composition. In the 5:1 sample, the band at 770 cm^{-1} shifts further to 762 cm^{-1} with a slight decrease in bandwidth, while the bands at 885 and 829 cm^{-1} are no longer apparent.

In the LPEI:LiTf system in this region, the 20:1 composition appears very similar to that of pure LPEI. As the concentration of LiTf is increased, the sharp bands at 855 and 883 cm^{-1} broaden and decrease in intensity until they are no longer distinguishable at the 5:1 composition. The LPEI band at 800 cm^{-1} is subsumed under a much broader, asymmetric band as in the LPEI:LiSbF₆ system. However, the center of this feature seems to occur at a somewhat higher frequency than in the LPEI:LiSbF₆ system at the same compositions. The small sharp peak at 757 cm^{-1} is due to the symmetric CF_3 deformation mode of the triflate anion.

The temperature-dependent spectra of the two LPEI-salt systems at a 20:1 composition over a temperature range from room temperature to 80 °C (well above the melting point of crystalline LPEI at ~65 °C) are shown in Figure 6 for the same spectral region shown in Figure 5. The spectra of pure LPEI at room temperature and 70 °C are also shown for comparison. However, the room temperature spectra of LPEI:LiTf and LPEI:LiSbF₆ are indistinguishable from their 35 and 40 °C spectra, respectively, and are not shown. In the 40 °C spectrum of LPEI:LiSbF₆ sample, in addition to the clearly defined bands at 883, 855, and 800 cm^{-1} , there is the additional band at 829 cm^{-1} that was observed in the 10:1 composition in Figure 5. At 65 °C, the 800 cm^{-1} band shifts and is seen as a very broad feature centered at roughly 763 cm^{-1} . There is also a broad band centered at 885 cm^{-1} . There appears to be little or no change in the spectrum upon heating to 80 °C. In general, the spectral behavior in this region over the temperature range from room temperature to 80 °C is strikingly

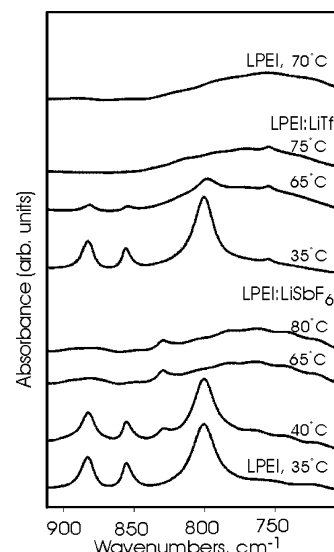


Figure 6. FT-IR spectra of the NH out-of-plane bending and CH_2 rocking modes of pure LPEI at 70 °C; LPEI:LiTf 20:1 at 75, 65, and 35 °C; LPEI:LiSbF₆ 20:1 at 80, 65, and 40 °C; and pure LPEI at 35 °C.

similar to the behavior observed over a composition range up to N:Li = 5:1, with higher temperature correlating to higher salt concentration. Of particular interest is the new peak at 829 cm^{-1} , which is the only sharp band of significant intensity persisting in this region at 80 °C.

A similar trend is seen in Figure 6 for the LPEI:LiTf 20:1 composition: as the temperature increases, the same types of spectral changes are seen as when the LiTf concentration is increased. Also note the spectrum of pure LPEI at 70 °C (above the melting temperature), which appears very similar to the LPEI salt systems at high salt concentration or elevated temperature. The band at 829 cm^{-1} appears only in the LPEI:LiSbF₆ system.

4. Ion-Ion and Ion-Polymer Interactions. The cation-anion interactions in the LPEI:salt complexes can be probed by examining those anion intramolecular modes whose frequencies and intensities are sensitive to coordination with cations. The SO_3 symmetric stretching mode, $\nu_s(\text{SO}_3)$, and the CF_3 symmetric deformation mode, $\delta_s(\text{CF}_3)$, of the triflate ion have been extensively used to study cation-anion interactions in lithium and sodium triflate complexed with poly(ethylene oxide) and oligomeric poly(ethylene oxide)^{3,15,27-29,31,35,36} and, more recently, studies of cation-anion interactions in LPEI²⁰ and in a monomeric LPEI model compound.³⁷ The IR spectra in the $\nu_s(\text{SO}_3)$ region of the LPEI:LiTf system at compositions of 20:1 and 5:1 near room temperature and well above the melt of LPEI are shown in Figure 7. In this region there is also a band at 1049 cm^{-1} in pure LPEI at room temperature, arising from mixed CH_2 twisting and NH bending modes, which disappears between 50 and 70 °C. As the salt concentration is increased from 20:1 to 5:1, the $\nu_s(\text{SO}_3)$ mode changes from a single band at 1031 cm^{-1} to two bands, at 1031 and 1036 cm^{-1} (indicated by the dashed lines). The growth of the band at 1036 cm^{-1} indicates that the speciation is changing from "free", or solvent-separated, triflate ions at the lower concentration to a mixture of "free" ions and ion pairs at the higher concentration. This figure also compares the two compositions as a function of temperature. Surprisingly, as the tempera-

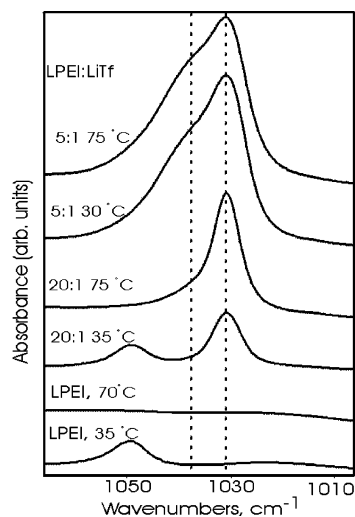


Figure 7. FT-IR spectra of LPEI:LiTf 5:1 and LPEI:LiTf 10:1 at 70 and 30 °C and pure LPEI at 70 and 35 °C in the region showing the SO_3 symmetric stretch of the triflate anion.

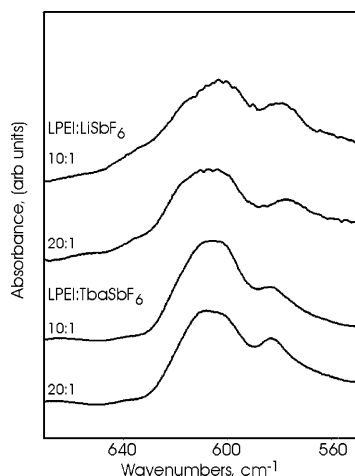


Figure 8. FT-IR spectra of the $\nu_3(\text{F}_{1\text{u}})$ mode of LPEI:LiSbF₆ 10:1 and 20:1 and LPEI:TbaSbF₆ 10:1 and 20:1.

ture is increased from 30 to 75 °C there appears to be no change in the speciation at any composition, as is indicated by the invariance of the intensities and frequencies of the bands at a given composition as the temperature is increased. The same speciation trends (an increase in aggregation with increasing salt concentration, but no effect with increasing temperature) are observed in the $\delta_s(\text{CF}_3)$ mode (not shown), in which the band center shifts from 753 to 758 cm^{-1} over the composition range.

Infrared spectra of two LPEI:LiSbF₆ complex from 500 to 700 cm^{-1} are shown in Figure 8. The $\nu_3(\text{F}_{1\text{u}})$ mode of the isolated SbF₆[−] ion is measured at 669 cm^{-1} in the IR spectrum of the pure LiSbF₆ crystal.³⁸ In the 20:1 LPEI:LiSbF₆ complex there are two prominent bands at 611 and 577 cm^{-1} that are also present in the 5:1 complex. This rather substantial frequency shift and the appearance of two bands resulting from the breaking of the degeneracy of the $\text{F}_{1\text{u}}$ mode of the SbF₆[−] anion at first suggests a strong interaction of the lithium ion with the SbF₆[−] ion. However, also shown in the figure are two spectra of tetrabutylammonium hexafluoroantimonate (TbaSbF₆) complexed with LPEI. This cation is quite bulky, and the positive charge is localized in a sterically protected core. Therefore, cation–anion interactions in complexes containing this cation are

expected to be negligible as studies of TbaTf in ethylene oxide and ethylenimine systems have verified.^{37,39} In LPEI:TbaSbF₆, the SbF₆[−] frequencies occur at 605 and 583 cm^{-1} in the 20:1 complex and are almost unchanged in the 5:1 complex. It is surprising that the SbF₆[−] bands in the LPEI:TbaSbF₆ complex occur at almost the same frequencies as in the LPEI:LiSbF₆ complexes, and both are significantly shifted from isolated ion values. These data show that it is not a cation–anion interaction that is responsible for the frequency shift. Coupled with the shift in the NH bending frequency seen in Figures 3 and 4, it seems reasonable to explain these data in terms of a hydrogen-bonding interaction of the SbF₆[−] anion with the NH of the LPEI backbone.

Conclusions

The behavior of the polymer bands in all spectral regions is almost identical with either increasing salt concentration or increasing temperature: the disappearance of numerous, relatively sharp bands and their replacement by a few, broad spectral features. The fact that this behavior is observed in both LiTf and LiSbF₆ complexes at identical compositions shows that the lithium ion is responsible for the striking spectral changes that reflect significant disordering of the system. The disordering occurs through a strong coordinative interaction with the nitrogen atom in the LPEI backbone that disrupts the hydrogen-bonding interaction in the crystalline LPEI structure. With either increasing temperature or increasing lithium ion coordination, the disruption of $\text{N}-\text{H} \cdots \text{N}$ hydrogen bonding undoubtedly results in an increase in structural disorder. This effect appears to be amplified in the spectra due to the extensive coupling of N–H bending motions with the chain stretching, bending, and deformation motions comprising the vibrational modes in the mid-IR. Therefore, disruption of hydrogen bonding throughout the polymer matrix is reflected in the dramatic collapse of a “sharp” vibrational mode structure.

In the LPEI:LiTf system there is an increase in cation–anion aggregation with increasing concentration, but no difference in cation–anion interaction with increasing temperature. In the LPEI:LiSbF₆ system, it appears that the primary interaction of the anion is with the NH group in the polymer backbone. This is apparent from the significant shift in the $\nu_3(\text{F}_{1\text{u}})$ mode of the SbF₆[−] ion, the appearance of the new NH bending band at 1550 cm^{-1} , and the new NH stretching band at 3238 cm^{-1} in the LPEI:LiSbF₆ spectra. The same behavior does not occur in the LPEI:LiTf spectra or the LPEI spectrum.

Acknowledgment. This work was supported by the National Science Foundation under Grant No. DMR-0072544. We thank Mr. Michael Erickson for synthesizing the LPEI.

References and Notes

- (1) Fenton, D. E.; Parker, J. M.; Wright, P. V. *Polymer* **1973**, *14*, 589.
- (2) Gauthier, M.; Bélanger, A.; Kapfer, B.; Vassort, G.; Armand, M. In *Polymer Electrolyte Reviews*; MacCallum, J. R., Vincent, C. A., Eds.; Elsevier: London, 1989; Vol. 2.
- (3) Chintapalli, S.; Frech, R. *Electrochim. Acta* **1995**, *40*, 2093–2099.
- (4) Ratner, M. A.; Shriver, D. F. *Chem. Rev.* **1988**, *88*, 109–124.
- (5) Allcock, H. R.; Napierala, M. E.; Olmeijer, D. L.; Best, S. A.; Merz, K. M., Jr. *Macromolecules* **1999**, *32*, 732–741.

- (6) Shriver, D. F.; Dupon, R.; Stainer, M. *J. Power Sources* **1983**, *9*, 383–388.
- (7) Bruce, P. G.; Vincent, C. A. *J. Chem. Soc., Faraday Trans.* **1993**, *89*, 3187–3203.
- (8) MacCallum, J. R.; Vincent, C. A. In *Polymer Electrolyte Reviews*; MacCallum, J. R., Vincent, C. A., Eds.; Elsevier: New York, 1987; Vol. 1.
- (9) Bruce, P. G.; Vincent, C. A. *Solid State Ionics* **1990**, *40–41*, 607–611.
- (10) *Polymer Electrolyte Reviews*; MacCallum, J. R., Vincent, C. A., Eds.; Elsevier Applied Science: New York, 1987; Vol. 1.
- (11) *Polymer Electrolyte Reviews*; MacCallum, J. R., Vincent, C. A., Eds.; Elsevier Applied Science: New York, 1989; Vol. 2.
- (12) Bruce, P. G. In *Polymer Electrolyte Reviews*; MacCallum, J. R., Vincent, C. A., Eds.; Elsevier Applied Science: New York, 1987; Vol. 1.
- (13) Berthier, C.; Gorecki, W.; Minier, M. *Solid State Ionics* **1983**, *11*, 91–95.
- (14) Frech, R.; Huang, W. *Macromolecules* **1995**, *28*, 1246–1251.
- (15) Frech, R.; Huang, W.; Dissanayake, M. A. K. L. *Mater. Res. Soc. Symp. Proc.* **1995**, *369*, 523–534.
- (16) Frech, R.; Chintapalli, S.; Bruce, P. G.; Vincent, C. A. *Chem. Commun.* **1997**, 157–158.
- (17) Frech, R.; Chintapalli, S.; Bruce, P. G.; Vincent, C. A. *Macromolecules* **1999**, *32*, 808–813.
- (18) Lightfoot, P.; Mehta, M. A.; Bruce, P. G. *Science* **1993**, *262*, 883–885.
- (19) Papke, B. L.; Ratner, M. A.; Shriver, D. F. *J. Electrochem. Soc.* **1982**, *129*, 1434–1438.
- (20) York, S.; Frech, R.; Snow, A.; Glatzhofer, D. *Electrochim. Acta* **2001**, *46*, 1533–1537.
- (21) Chiang, C. K.; Davis, G. T.; Harding, C. A.; Takashi, T. *Macromolecules* **1985**, *18*, 825–827.
- (22) Chiang, C. K.; Davis, G. T.; Harding, C. A.; Takashi, T. *Solid State Ionics* **1986**, *18&19*, 300–305.
- (23) Harris, C. S.; Shriver, D. F.; Ratner, M. A. *Macromolecules* **1986**, *20*, 1778–1781.
- (24) Harris, C. S.; Ratner, M. A.; Shriver, D. F. *Macromolecules* **1987**, *20*, 1778–1781.
- (25) Tanaka, R.; Fujita, T.; Nishibayashi, H.; Saito, S. *Solid State Ionics* **1993**, *60*, 119–123.
- (26) Gadjourova, Z.; Marero, D. M.; Andersen, K. H.; Andreev, Y. G.; Bruce, P. G. *Chem. Mater.* **2001**, *13*, 1282–1285.
- (27) Frech, R.; Huang, W. *Solid State Ionics* **1994**, *72*, 103–107.
- (28) Huang, W.; Frech, R.; Johansson, P.; Lindgren, J. *Electrochim. Acta* **1995**, *40*, 2147–2151.
- (29) Muhuri, P. K.; Das, B.; Hazra, D. K. *J. Phys. Chem. B* **1997**, *101*, 3329–3332.
- (30) Frech, R.; Rhodes, C. P.; York, S. S. *Mater. Res. Soc. Symp. Proc.* **1999**, *548*, 335–345.
- (31) Peterson, G.; Jacobsson, P.; Torell, L. M. *Electrochim. Acta* **1992**, *37*, 1495–1497.
- (32) Chatani, Y.; Kobatake, T.; Tadokoro, H.; Tanaka, Y. *Macromolecules* **1982**, *15*, 170–176.
- (33) Boesch, S. E.; York, S. S.; Frech, R.; Wheeler, R. A. *Phys. Chem. Comm.* **2001**, *1*.
- (34) Sanders, R. A.; Frech, R.; Khan, M. A. *J. Phys. Chem. B*, submitted for publication.
- (35) Ferry, A. *J. Phys. Chem. B* **1997**, *101*, 150–157.
- (36) Rhodes, C. P.; Frech, R. *Solid State Ionics* **2000**, *136–137*, 1131–1137.
- (37) York, S. S.; Boesch, S. E.; Wheeler, R. A.; Frech, R. *Phys. Chem. Commun.* **2002**, 99–111.
- (38) Begun, G. M.; Rutenberg, A. C. *Inorg. Chem.* **1967**, *6*, 2212–2216.
- (39) Frech, R.; Huang, W. *J. Solution Chem.* **1994**, *23*, 469–481.

MA030478Y